Development of a LaB_6 Cathode for High-Power Hall Thrusters

IEPC-2015-47／ISTS-2015-b-47

Presented at Joint Conference of 30th International Symposium on Space Technology and Science, 34th International Electric Propulsion Conference and 6th Nano-satellite Symposium
Hyogo-Kobe, Japan
July 4–10, 2015

Daniela Pedrini*
University of Pisa, Pisa, 56126, Italy

Riccardo Albertoni†
SITAEL S.p.A., Ospedaletto, Pisa, 56121, Italy

Fabrizio Paganucci‡
University of Pisa, Pisa, 56126, Italy

and

Mariano Andrenucci§
SITAEL S.p.A., Ospedaletto, Pisa, 56121, Italy

Abstract: High-power Hall effect thrusters represent attractive propulsion systems to perform thrust-intensive and deep-space missions. For this class of thrusters the cathodes must be able to sustain operating currents up to several tens of amperes. To this purpose, a heaterless lanthanum hexaboride (LaB_6) cathode for 5-kW-class Hall effect thrusters has been developed and tested at SITAEL S.p.A. (formerly Alta S.p.A.). The boride compound has been selected for the longer expected lifetime at the required discharge current, despite the higher work function as compared to the traditional dispenser emitters. In addition, a LaB_6 cathode relaxes the gas purity requirements due to a reduced sensitivity to contaminants and does not require a lengthy conditioning process to initiate the electron emission. The cathode design features a refractory metal tube and a graphite keeper to limit the effect of sputtering by ion bombardment on this electrode. A laboratory model of the cathode was experimentally characterized using both xenon and krypton as propellants. The cathode was tested at current levels as high as 18 A for a total of about 340 hours of continuous operation and more than 100 cold ignitions. The cathode was also coupled with the 5-kW HT5k Hall thruster, showing a successful operation and good performance. The experimental results will be presented and compared with the predictions from a previously developed model describing the operation of thermionic hollow cathodes, showing a good agreement between empirical and theoretical data.

*PhD Candidate, Department of Civil and Industrial Engineering, daniela.pedrini@for.unipi.it.
†Project Manager, Space Propulsion Business Unit, riccardo.albertoni@sitael.com.
‡Associate Professor, Department of Civil and Industrial Engineering, f.paganucci@ing.unipi.it.
§Space Propulsion Business Unit Manager, mariano.andrenucci@sitael.com.

I. Introduction

The interest in high-power Hall effect thrusters is increasingly fostered by the demand of space missions to provide high-thrust, long-lived propulsion systems. The benefits provided by electric propulsion (EP) are tied to a lower propellant mass with respect to chemical propulsion, allowing for a higher payload mass, a lower total mass, therefore less expensive launch vehicles[1]. The telecommunication industry can take advantage of the use of electric thrusters, since station-keeping and orbit-raising maneuvers are enabled by the availability of high power onboard telecommunication satellites. EP systems can lead to cost savings also in the field of deep-space missions, as demonstrated by Deep Space 1, SMART-1, Hayabusa, and Dawn[2–5]. In addition, new mission concepts would require very high levels of electric power (up to 300 kW) for the in-space transportation of large masses[6]. In this perspective, high-power Hall thrusters are of primary interest for the space community.

The next-generation Hall thrusters will require hollow cathodes suited to high-power applications, capable of providing high discharge currents and long life[7]. In this context, a lanthanum hexaboride (LaB_6) hollow cathode for 5-kW Hall thrusters has been developed and tested at SITAEL, Space Propulsion Business Unit (formerly Alta). The cathode is required to provide discharge currents in the 8-20 A range with lifetime in excess of 10000 hours. The low-current cathode design previously developed at SITAEL has been adapted to the high-current range. A heaterless configuration has been selected, promoting the removal of the single-point failure represented by the heater. The major drawback of this choice lies on the higher voltages required to ignite the cathode, and to possible thermal shocks damaging the LaB_6 emitter. The LaB_6 compound has been selected for the high robustness, high current density and long life of the emitters, with respect to the traditional dispenser cathodes. Dispenser emitters feature a tungsten matrix impregnated with barium-based mixtures and rely on chemical reactions to form a low-work-function surface layer[8]. They are thus susceptible to poisoning that can increase the work function or even hinder the cathode operation. A LaB_6 emitter does not require lengthy activation procedures and has a low sensitivity to contaminants and air exposure, increasing the cathode reliability. The main disadvantage of LaB_6 with respect to dispenser emitters is the higher work function, which is between 2.4 and 2.7 eV for polycrystalline LaB_6 cathodes[9,10] compared to about 2.1 eV for dispenser cathodes[8]. This property directly translates into an operating temperature of about 1650 °C for LaB_6 compared to about 1050 °C for a dispenser emitter, to give a current density in the order of 10^5 A/m^2. This consideration constitutes a non-negligible issue for the thermal design of low-current cathodes, since high temperatures in a small device must be tolerated by the materials without deterioration of the thermal and mechanical properties. Oppositely, the higher temperatures associated with the use of a LaB_6 emitter can be more easily handled in the design of a high-current cathode, given the availability of larger surfaces for the heat transfer mechanisms.

The cathode was characterized with both xenon and krypton propellants. The interest in krypton is tied to the reduction of on-ground development and qualification costs, and also to relax the dependence on the volatile natural-resource market[11]. A successful operation of the cathode was observed with both propellants in the investigated range of operating conditions, with no substantial damages detected during a partial post-test inspection. The experiments proved the reliability and robustness of the design in terms of ignition procedure, discharge parameters and steady-state temperatures.

II. Cathode Design

Following the traditional architecture[8], the hollow cathode is made of a 9 mm-diameter refractory tube housing a polycrystalline LaB_6 emitter or insert acting as an electron source (Fig. 1). Gas propellant is flowed through the tube and is ionized by the emitted electrons producing the internal plasma to sustain the discharge. The tube is machined in such a way to end with an orificed section against which the insert is pushed by means of a tungsten spring. The hole has a length-to-diameter aspect-ratio of about 1.2 and was obtained through electrical-discharge tube machining. The insert is shaped as a hollow cylinder 3.6 mm in inside diameter and 25 mm in length, thus providing an available area of about 280 mm^2 for the electron emission. Given the reactivity of LaB_6 with many refractory metals at high temperature, graphite sleeves are interposed between the insert and the tube to create a barrier handling this compatibility issue. For the same reason, several graphite spacers are placed between the insert and the spring. This choice allows also for distancing the spring from the hottest part of the tube, with a consequent operation at lower temperatures hindering the deterioration of the mechanical properties of tungsten. The cathode tube is made of TZM

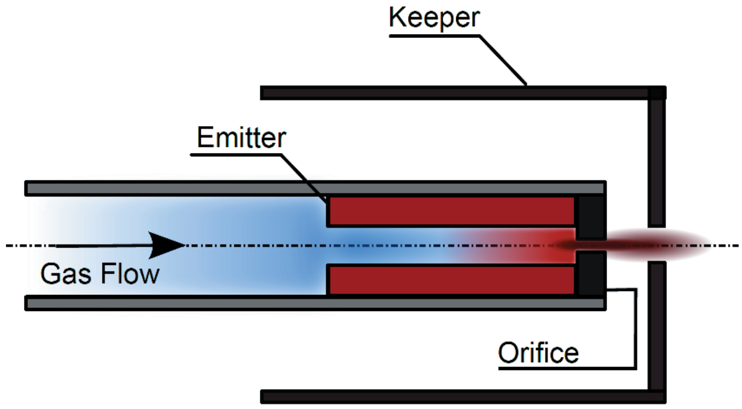

Figure 1. General scheme of an orificed hollow cathode.

molybdenum alloy, which shows good machinability and thermal properties for the present application (e.g. higher ductility and lower thermal conductivity with respect to pure molybdenum). The cathode tube is surrounded by the keeper electrode, which is shaped as an external tube in an enclosed configuration. The keeper features an orifice in its exit section, whose diameter is approximately twice the diameter of the main tube orifice. The keeper is used to ease the cathode ignition by means of an applied positive potential with respect to the inner tube and to protect the cathode orifice from ion bombardment. On the basis of electrostatic simulations, an inter-electrode distance of 2 mm was selected in the longitudinal direction to produce reliable ignitions. Given the lower sputtering yield with respect to metals, graphite was selected as the keeper material to limit the damage due to ion bombardment on this electrode. Insulation among the various parts of the cathode kept at different potentials was guaranteed by BN components, whose dielectric strength prevented the possibility of short circuits in the assembly. The laboratory model of the cathode was provided with screws to easily disassemble the components.

The described geometry derives from the suggestions obtained from a previously developed numerical model, which proved to be a useful tool to guide the design of thermionic hollow cathodes[12]. Successful test campaigns carried out at SITAEL on low-current LaB_6 cathodes[13] have shown a satisfactory cathode operation and suggested improvements to upgrade the theoretical model[14]. The high-current numerical results have been compared with the related experimental data, as shown in Section IV.

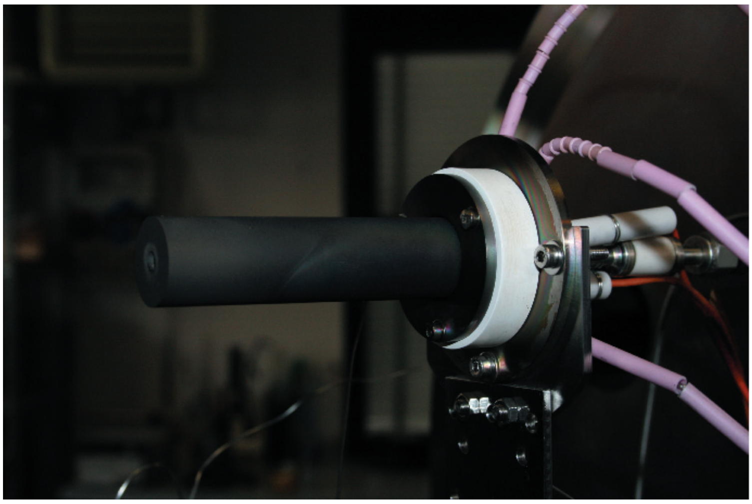

Figure 2. Cathode setup in the SITAEL IV1 facility.

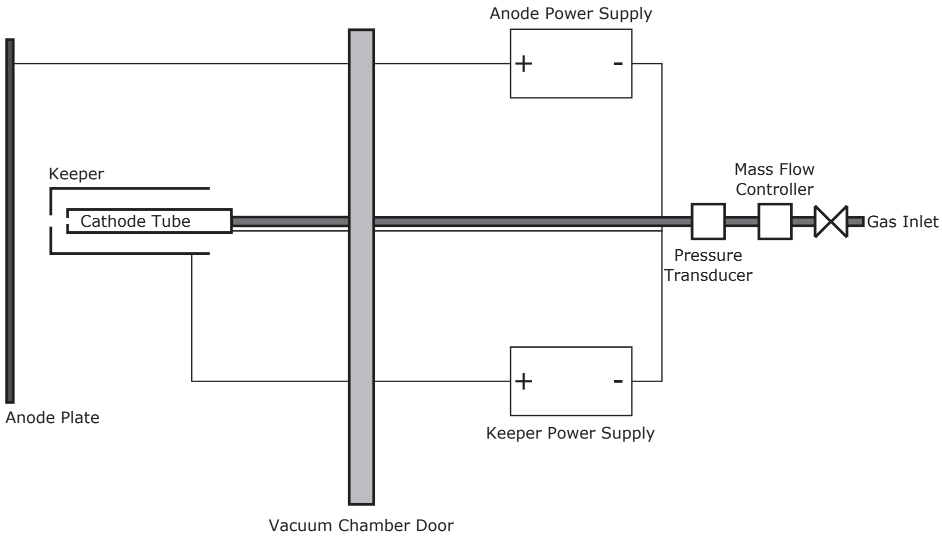

Figure 3. Schematic of the electrical circuit for the cathode in the IV1 vacuum chamber.

III. Experimental Equipment

The experimental activities were carried out in two phases. Firstly, the cathode was tested at SITAEL in the IV1 vacuum chamber, which was equipped with an anode plate to carry out the characterization. Subsequently, an experimental campaign of the cathode with the 5-kW HT5k Hall thruster[11] was performed in the SITAEL IV10 facility to assess the performance and address the possible coupling problems.

A. Test Facility

The IV1 facility consists of a cylindrical stainless steel body 600 mm in diameter and 1600 mm in length. The test bench is equipped with a primary scroll pump, a 300 l/s turbo molecular pump and two 900 l/s cryogenic pumps. The facility is able to reach a background pressure of 1×10^{-6} Pa when the combined pumping system is activated. The pressure level within the chamber is continuously monitored by two Leybold-Inficom IT90 Pirani/Bayard-Alpert sensors and recorded via LabVIEW DAQ. The cathode setup in the IV1 chamber is shown in Fig. 2.

The IV10 vacuum chamber is made of a cylindrical stainless steel body 5740 mm in diameter and 9400 mm in length. The facility is equipped with two 2000 l/s turbo molecular pumps, two scroll pumps, two 5000 l/s cryogenic pumps and five 60000 l/s cold panels. The ultimate vacuum in the chamber is as low as 10^{-9} mbar, whereas the operating vacuum is in the order of 10^{-6} mbar at 3.6 mg/s Xe.

B. Propellant and Power Systems

Figure 3 schematically depicts the electrical circuit of the experimental arrangement in the IV1 facility. A current-limited Huttinger PFG5000 (1000 V, 6 A) power supply controlled the cathode-to-keeper voltage during discharge initiation and the current during operation. An external anode plate located 70 mm downstream of the cathode was used for the diode-mode operation. The cathode-to-anode current was controlled using a Sorensen DLM 150-20E (150 V, 20 A) power supply. Both power supplies were connected to a common negative reference and the set-up was electrically floating with respect to ground. High purity (grade N48) xenon and krypton were used during the test campaigns. K-type thermocouples were installed on the mounting flange constituting the mechanical interface, on the outer keeper flange and on the backside of the anode. In addition, two B-type thermocouples suited for measurements up to 1800 °C were installed on the external surface of the cathode main tube at 12 and 41 mm upstream of the tip.

During the coupling test with the HT5k, the cathode-to-keeper voltage was controlled by a Magna-Power XR1000-6.0 (1000 V, 6 A) power supply, whereas the cathode-to-anode current was controlled by a Magna-Power TSD400-36 (400 V, 36 A) power supply.

IV. Results and Discussion

The experiments were aimed at characterizing the hollow cathode with both xenon and krypton as propellants, mapping the performance variations as a function of the operating conditions in terms of discharge current and mass flow rate. The cathode ignition was also investigated in order to select a reliable procedure and sequence of operations. A 300-hours endurance test with xenon was performed and its effects on the cathode characteristics were evaluated. In addition, the temperature measurements were useful to monitor the structural integrity of the materials and for a comparison with theoretical data to check the accuracy of the model.

The cathode showed a reliable ignition, a stable and low discharge voltage, and allowed for a successful thruster operation without experiencing major issues.

A. Cathode Ignition

Since the hollow cathode was tested in a heaterless configuration, the applied keeper voltage needed to initiate the discharge was expected to be several hundred volts higher than typical values of corresponding heated cathodes. This is a natural consequence of the lack of a prior heating phase of the insert, which would permit a significant thermionic electron emission due to an increased surface temperature thus lowering the required voltage for the plasma breakdown.

The ignition procedure consisted in applying 800 V to the keeper and 130 V to the anode. The keeper current was regulated to 2 A and the anode current was set to 16 A. A mass flow rate of 5 mg/s was then flowed through the cathode, which was run at a total current of 18 A for about 30 minutes before starting each characterization test. Immediately after the discharge initiation, the mass flow rate was smoothly reduced to 1 mg/s in a couple of minutes. After the cathode shutdown, the propellant was flowed for 10-15 minutes to force the cooling of the emitter and to prevent oxygen contamination at high temperatures. More than 100 cold ignitions were accumulated during the cathode characterization.

B. Cathode Performance

For a given current level, the parameters of major interest for the assessment of the cathode performance are the power consumption and the minimum mass flow rate ensuring the spot-mode operation. As reported by Fearn[15], two main operating modes have been revealed for the cathode operated in diode configuration. Depending on the discharge current and mass flow rate, regions of spot and plume mode can be distinguished. The plume mode is characterized by high voltages and electrical noise, with a highly luminous discharge

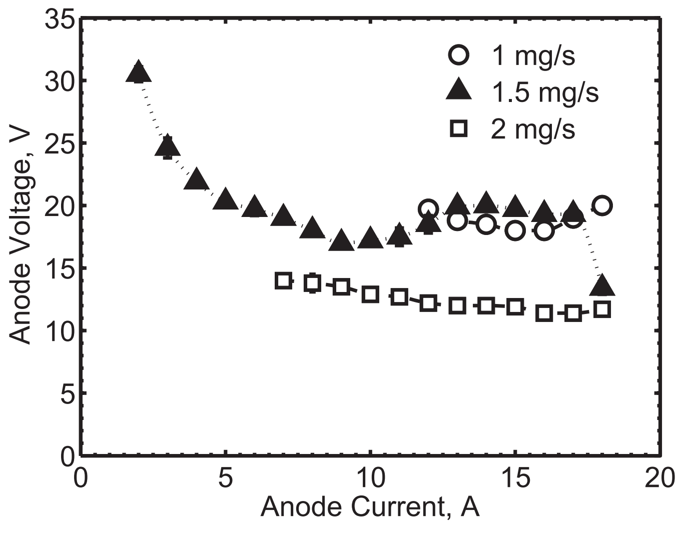

Figure 4. Anode voltage versus anode current, pre-endurance Xe operation, floating keeper.

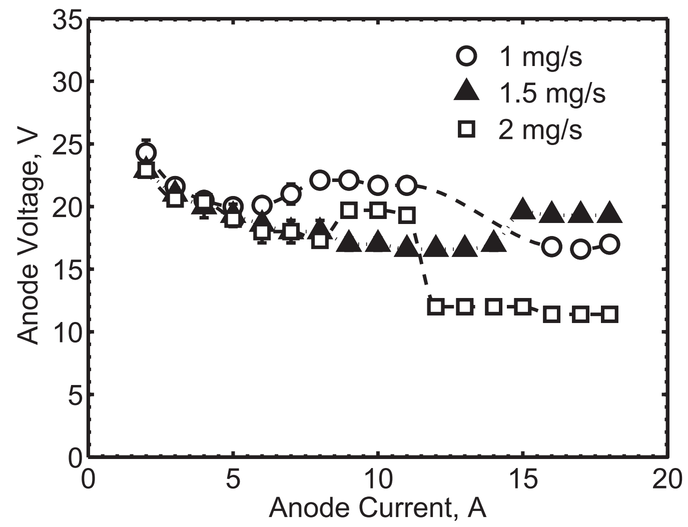

Figure 5. Anode voltage versus anode current, post-endurance Xe operation, floating keeper.

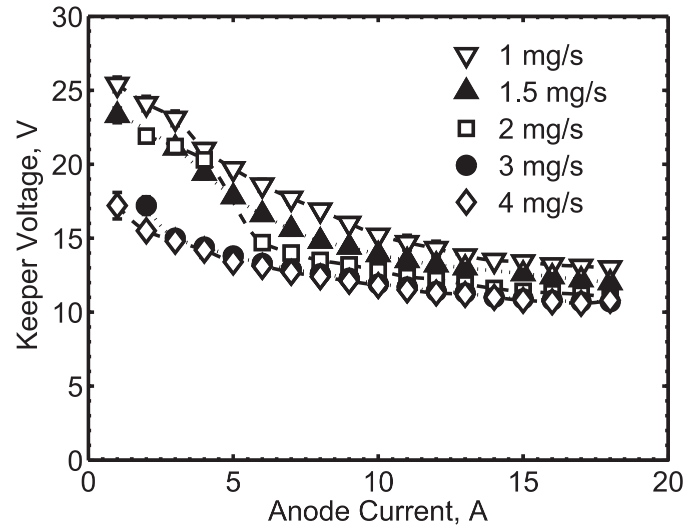

Figure 6. Keeper voltage versus anode current, post-endurance Xe operation, 2 A keeper current.

around the cathode tip. This mode is encountered when the mass flow rate is reduced to low values while keeping the current fixed. As the mass flow rate is increased, a sudden transition occurs to the spot mode, where the voltage remains stable and low, and the radiation is only emitted from the cathode orifice.

The power consumption is defined by the discharge voltage drop and is linked to the choice of the relevant geometrical parameters of the cathode. A balance is sought between the performance parameters when defining the length and diameter of both the insert and the orifice. As a matter of fact, increasing the orifice diameter allows for a lower ohmic drop in the orifice region and a better use of the insert, which is tied to a reduced internal pressure entailing a deeper plasma penetration in the cathode interior. However, a larger orifice is not favorable to ensure the spot mode at low flow rates, showing that a tradeoff exists in selecting the cathode geometry[16].

Referring to the diode operation with the anode plate, the cathode performance was investigated before and after a 300-hours endurance test at 1 mg/s Xe and 16 A anode current, being the keeper floating. After the endurance test, the cathode was also fed with krypton propellant to draw a performance comparison

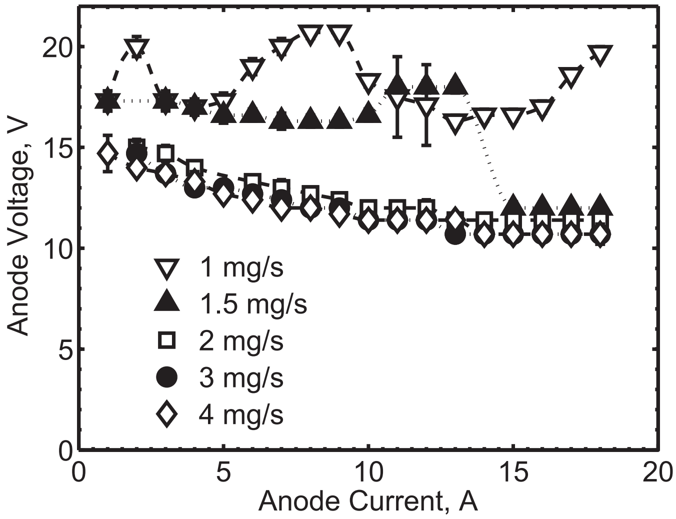

Figure 7. Anode voltage versus anode current, post-endurance Xe operation, 2 A keeper current.

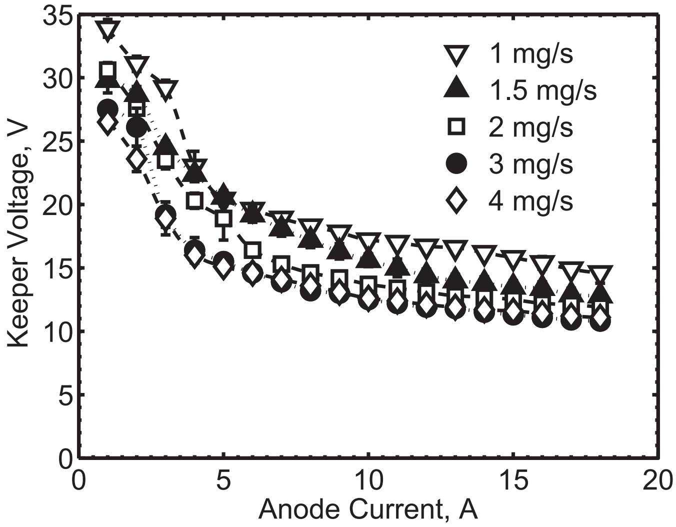

Figure 8. Keeper voltage versus anode current, post-endurance Kr operation, 2 A keeper current.

with the xenon operation. For a given mass flow rate, two sweeps through the selected current range were performed, keeping the cathode at each level of current for 5 minutes. The error bars reported in the figures show the standard deviation found in the data collected when increasing and decreasing the current. Figures 4 and 5 refer to the electrical characteristics of the cathode with floating keeper at three xenon mass flow rates, before and after the endurance test, respectively. In almost all cases the post-endurance anode voltage was from 1 to 5 V lower than the pre-endurance values. The sudden voltage drops reported in the figures may be tied to a transition from plume to spot mode, occurring from 17 to 18 A at 1.5 mg/s in Fig. 4 and from 11 to 12 A at 2 mg/s in Fig. 5. The post-endurance keeper voltage and anode voltage as a function of anode current with a fixed keeper current of 2 A at five xenon mass flow rates are respectively shown in Fig. 6 and Fig. 7. In accordance with experimental results found in the literature[7,17,18], lower voltages were measured at higher mass flow rates. Attempts to extract an anode current lower than 2 A, especially at the lower mass flow rates, caused the anode voltage to increase and the cathode to cool off, likely due to the

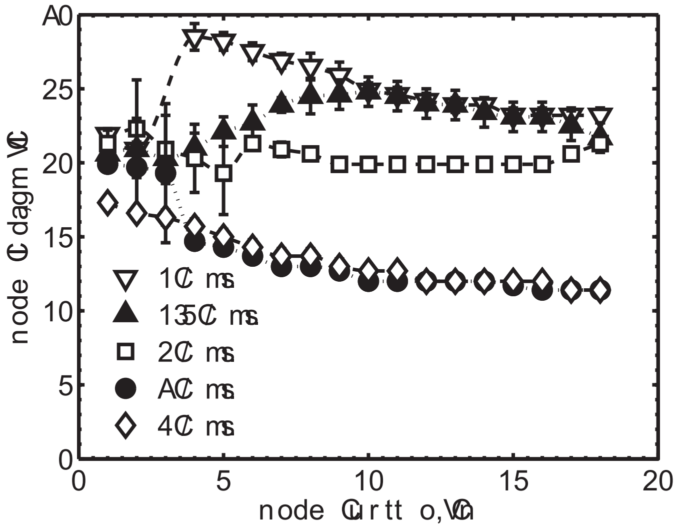

Figure 9. Anode voltage versus anode current, post-endurance Kr operation, 2 A keeper current.

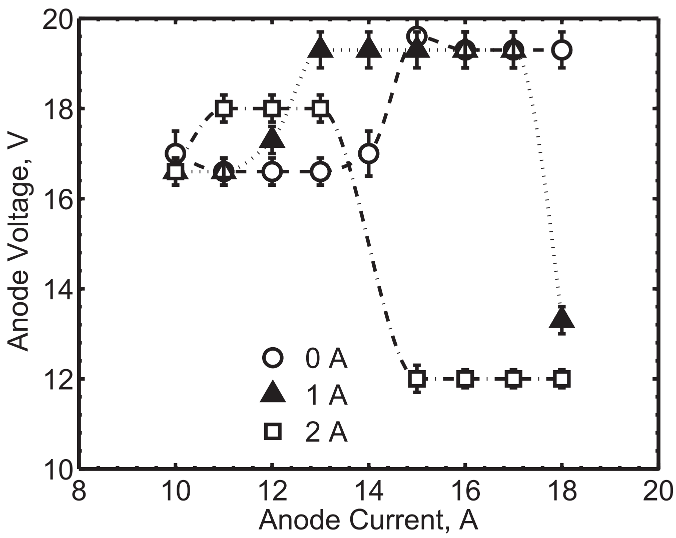

Figure 10. Anode voltage versus anode current at different keeper currents, post-endurance 1.5 mg/s Xe operation.

reduction in the self-heating by ion-bombardment. The anode voltage oscillations with the anode current at the lower mass flow rates might be tied to a less-efficient cathode-to-anode coupling leading to transitions between spot and plume mode, as already observed by Fearn[15].

Similar characteristics were reported for krypton operation, as shown in Fig. 8 and Fig. 9. Nevertheless, a less efficient ion production with respect to xenon entails a higher power consumption of up to 60 W with krypton as compared to the corresponding operating points with xenon.

The effect of the current collected by the keeper electrode was investigated and the relevant results are summarized in Fig. 10 for xenon and Fig. 11 for krypton, in both cases at 1.5 mg/s mass flow rate. The anode voltage proved to be insensitive to the keeper current range from 0 to 2 A in the case of krypton, whereas differences of up to about 8 V were observed with xenon.

The results of the theoretical model were compared with the experimental data, showing a good agreement

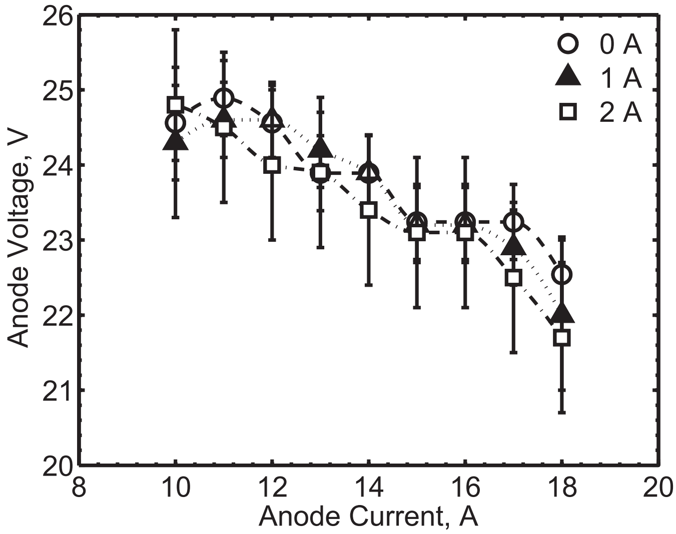

Figure 11. Anode voltage versus anode current at different keeper currents, post-endurance 1.5 mg/s Kr operation.

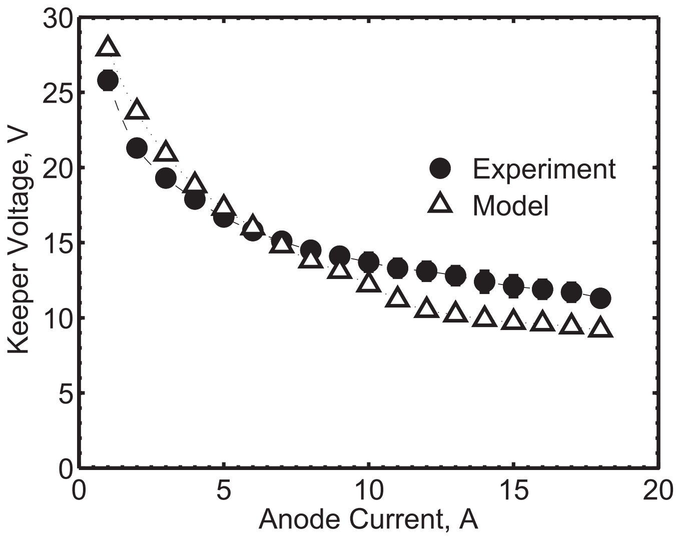

Figure 12. Comparison between experimental and theoretical characteristics, pre-endurance 1 mg/s Xe operation, 2 A keeper current.

of the electrical characteristics, both in the voltage values and in the general trends with the current. A representative example is reported in Fig. 12, where the pre-endurance keeper voltage as a function of anode current, at 2 A keeper current and 1 mg/s Xe, is compared with the corresponding numerical results. The figure shows that at lower currents the model over-estimates the keeper voltage, the opposite holding at higher currents. Nevertheless, the maximum discrepancy is about 3 V, and the model proved to predict the keeper voltage values with a difference lower than 20 %.

The temperatures at the relevant locations of the cathode assembly were monitored during the endurance test. The B-type thermocouple located in proximity of the active zone on the outer cathode tube surface recorded a value of 1168 ± 3 °C, the highest of the cathode assembly. Correspondingly, the second B-type thermocouple farther from the tube exit measured a temperature of 1114 ± 3 °C. The K-type thermocouples measured about 80 °C at the outer keeper flange surface, about 60 °C at the mounting flange and about

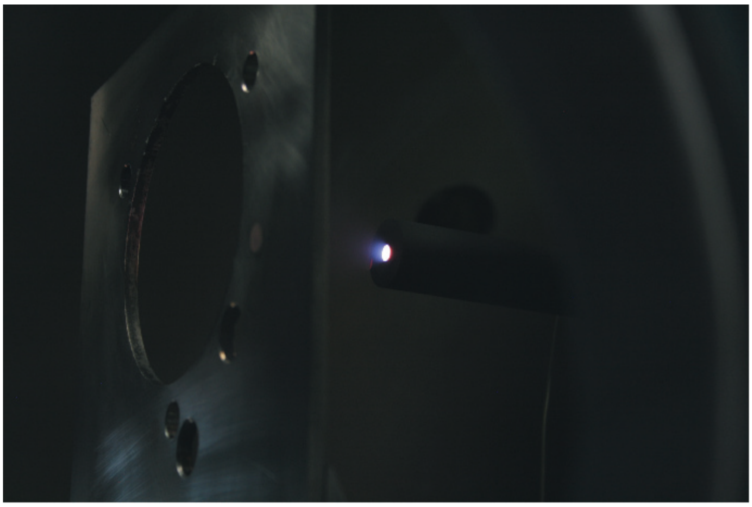

Figure 13. Hollow cathode operated with xenon in the IV1 facility.

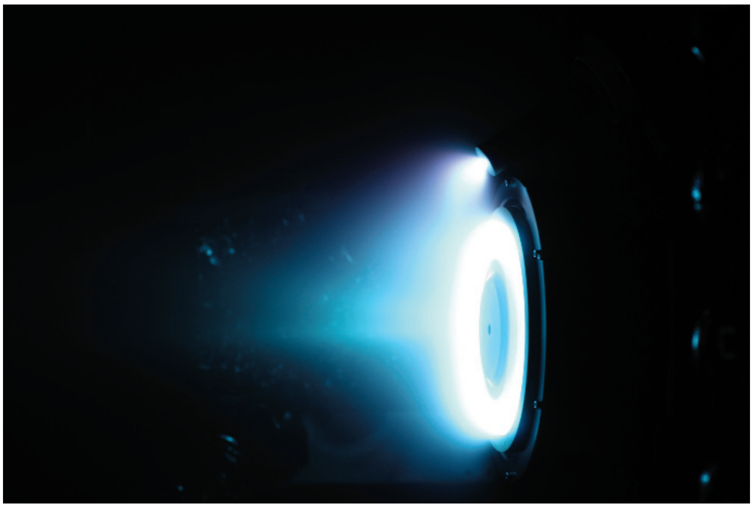

Figure 14. Cathode coupled with the HT5k Hall thruster in the IV10 facility.

30 °C at the anode plate.

At the operating conditions of the endurance test, the temperature computed with the aid of the thermal model in the global numerical code is about 1530 °C at the node in contact with the active zone of the insert. This means that the theoretical value is about 360 °C higher than the experimental one, meaning a difference in the order of about 27 %. This discrepancy suggests possible modifications in the theoretical model and in the thermal simulations, such as the inclusion of a proper contact resistance between the insert and the tube to yield a more realistic picture of the heat exchanges mechanisms between these two components. The temperature measured by the B-type thermocouple farther from the active zone is near the theoretical value of 1035 °C, thus the discrepancy is only about 7 %.

Figures 13 and 14 show the cathode operated with the anode plate and with the HT5k Hall thruster, respectively.

C. Post-Test Visual Inspection

The predominant factors in limiting the cathode lifetime include failure-to-start due to emitter contamination and keeper-to-cathode common shorting. Wear mechanisms such as orifice clogging along with erosion due

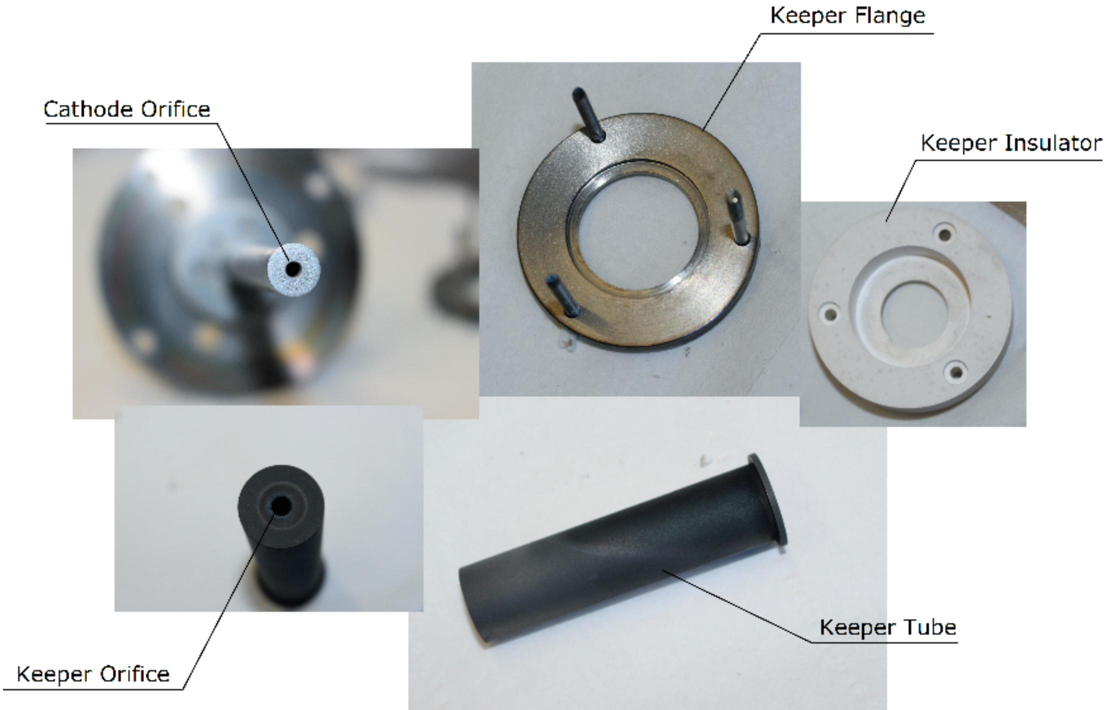

Figure 15. Post-test visual inspection.

to ion sputtering on both the orifice and the keeper are likely to promote a degradation in the cathode performance. The cathode was partially disassembled after approximately 340 hours of operation and more than 100 cold ignitions, to assess the effect of the extended operation. Optical inspections of the orifice, the cathode tube and the keeper assembly were carried out. As shown in Fig. 15, the cathode exit surface exhibits signs of erosion due to ion bombardment on its exterior. Nevertheless, the cathode orifice appears to be almost intact. The keeper orificed section also shows external circular patterns with surface color modifications caused by the interaction with the plasma discharge. The keeper orifice has been cleaned to remove a small quantity of graphite debris, which did not modify its circular shape. Looking at the lateral surface of the keeper, effects of the discharge are visible with a lighter color towards the downstream end of the tube. A small impedance degradation of the keeper-to-cathode insulation was experienced during the test, this effect being ascribed to deposition of either refractory metal from the cathode tube or graphite from the keeper, spacers and sleeves on the downstream surface of the insulator. As a matter of fact, an easily-removable layer deposited on the keeper insulator has been observed and removed during the post-test inspection. The metallic flange used to hold the keeper in place appears to be intact.

V. Conclusion

A heaterless LaB_6 hollow cathode was developed for high-current applications and tested with xenon and krypton. The cathode was characterized in diode configuration at anode currents from 2 to 18 A, and a 300 hours endurance test was performed at 16 A and 1 mg/s Xe. The cathode was also coupled with the HT5k Hall thruster, proving the reliability and flexibility of the design in terms of the operating envelope and cold ignitions. Improvements in the thermal and mechanical design of the cathode are in progress with the aim of reducing the power consumption, as well as to extend the spot-mode operation of the cathode.

Acknowledgments

The authors gratefully acknowledge the contribution of S. Gregucci and A. Hock for the laboratory activities in the IV1 facility, and C. Ducci, U. Cesari, N. Giusti and P. Balducci for the tests in the IV10 vacuum chamber.

References

[1]Oleson, S., and Meyer, R., "Launch Vehicle and Power Level Impacts on Electric GEO Insertion," AIAA-96-2978, 32^{nd} Joint Propulsion Conference, Washington DC, USA, 1996.

[2]Polk, J. E., et al., "Validation of the NSTAR Ion Propulsion System on the Deep Space One Mission: Overview and Initial Results," AIAA 99-2274, 35^{th} AIAA/ASME/SAE/ASEE Joint Propulsion Conference & Exhibit, 20-24 June 1999, Los Angeles, California, USA.

[3]Racca, G. D., "SMART-1 from Conception to Moon Impact," *Journal of Propulsion and Power*, Vol. 25, No. 5, September-October 2009, pp. 993-1002.

[4]Kuninaka, H., Nishiyama, K., Shimizu, Y., Hosoda, S., Koizumi, H., and Kawaguchi, J., "Status of Microwave Discharge Ion Engines on Hayabusa Spacecraft," AIAA 2007-5196, 43^{rd} AIAA/ASME/SAE/ASEE Joint Propulsion Conference & Exhibit, 8-11 July 2007, Cincinnati, OH, USA.

[5]Rayman, M. D., Fraschetti, T. C., Raymond, C. A., and Russell, C. T., "Dawn: A mission in development for exploration of main belt asteroids Vesta and Ceres," *Acta Astronautica*, Vol. 58, No. 11, pp. 605-616.

[6]Brophy, J. R., Gershman, R., Strange, N., Landau, D., Merrill, R. G., and Kerslake, T., "300-kW Solar Electric Propulsion System Configuration for Human Exploration of Near-Earth Asteroids," AIAA 2011-5514, 47^{th} AIAA/ASME/SAE/ASEE Joint Propulsion Conference & Exhibit, 31 July - 03 August 2011, San Diego, California, USA.

[7]Chu, E, and Goebel, D. M., "High-Current Lanthanum Hexaboride Hollow Cathode for 10-to-50-kW Hall Thrusters," *IEEE Transactions on Plasma Science*, Vol. 40, No. 9, September 2012, pp. 2133-2144.

[8]Goebel, D. M., and Katz, I., *Fundamentals of Electric Propulsion: Ion and Hall Thrusters*, John Wiley and Sons, NJ, USA, 2008.

[9]Lafferty, J. M., "Boride Cathodes," *Journal of Applied Physics*, Vol. 22, No. 3, pp. 299-309.

[10]Ahmed, H., and Broers, A. N., "Lanthanum Hexaboride Electron Emitter," *Journal of Applied Physics*, 43, 2185, 1972.

[11]Misuri, T., Pergola, P., and Andrenucci, M., "HT5k Hall Thruster to Improve Small Launcher Capabilities," IEPC-2013-279, 33^{rd} International Electric Propulsion Conference, 6-10 October 2013, Washington DC, USA.

[12]Albertoni, R., Pedrini, D., Paganucci, F., and Andrenucci, M., "A Reduced-Order Model for Thermionic Hollow Cathodes," *IEEE Transactions on Plasma Science*, Vol. 41, No. 7, June 2013, pp. 1731-1745.

[13]Albertoni, R., Andrenucci, M., Pedrini, D., and Paganucci, F., "Preliminary Characterization of a LaB6 Hollow Cathode for Low-Power Hall Effect Thrusters," IEPC-2013-137, 33^{rd} International Electric Propulsion Conference, 6-10 October 2013, Washington DC, USA.

[14]Pedrini, D., Albertoni, R., Paganucci, F., and Andrenucci, M., "Theoretical Model of a Lanthanum Hexaboride Hollow Cathode," *IEEE Transactions on Plasma Science*, Vol. 43, No. 1, November 2014, pp. 209-217.

[15]Fearn, D. G., and Patterson, S. W., "Characterisation of the High Current Hollow Cathode for the T6 Ion Thruster," 34^{th} AIAA/ASME/SAE/ASEE Joint Propulsion Conference & Exhibit, 13-15 July 1998, Cleveland, OH, USA.

[16]Pedrini, D., Albertoni, R., Paganucci, F., and Andrenucci, M., "Modeling of LaB6 Hollow Cathode Performance and Lifetime," *Acta Astronautica*, Vol. 106, pp. 170-178.

[17]Capacci, M., Minucci, M., and Severi, A., "Simple Numerical Model Describing Discharge Parameters in Orificed Hollow Cathode Devices," AIAA 1997-2791, 33^{rd} AIAA/ASME/SAE/ASEE Joint Propulsion Conference & Exhibit, 6-9 July 1997, Seattle, WA, USA.

[18]Domonkos, M. T., "Evaluation of Low-Current Orificed Hollow Cathodes," Ph.D. dissertation, Department of Aerospace Engineering, University of Michigan, Ann Arbor, MI, USA, 1999.